DESIGN AND BEAM DYNAMICS STUDY OF HYBRID ESS LINAC

M. Eshraqi, H. Danared, W. Hees, A. Jansson
European Spallation Source, Lund, Sweden

Abstract

The European Spallation Source, ESS, will use a superconducting linear accelerator delivering high current long pulses with an average beam power of 5 MW to the target station at 2.5 GeV. A new cryomodule architecture is proposed that can have a quasi-segmented interlacing which provides enough room for beam diagnostics, and can reduce the cryo heat load with respect to the segmented design by keeping the transition regions at sub-100 K region.

This paper will present a review of the LINAC design, beam dynamics studies and a preliminary cryogenic analysis of the transition region.

INTRODUCTION

The European Spallation Source, ESS, to be built in Lund, Sweden, will require a high current superconducting proton LINAC to accelerate protons to be used for the spallation process on which a high flux of pulsed neutrons will be generated. The accelerator is a 5 MW LINAC delivering proton beams of 2.5 GeV to the target in pulses of 2.86 ms long with a repetition rate of 14 Hz. Beam current is 50 mA, which at 352.21 MHz is equivalent to $\sim 9 \times 10^8$ protons per bunch. The latest design of the LINAC can be found at ref. [1] and the 2003 Design Update can be found at reference [2].

It is foreseen not to exclude the possibility of a potential upgrade of the LINAC to a higher power at the fixed energy of 2.5 GeV, by increasing the current. Increasing the beam current implies that in case of fixed power couplers the energy gain per cavity will decrease, to reach the fixed energy of 2.5 GeV, extra cryo-modules will be needed, to be installed in the current High Energy Beam Transport line.

SUPERCONDUCTING LINAC STRUCTURES

Two types of superconducting structures will accelerate the beam after the normal conducting DTL from 50 MeV to 2.5 GeV. The first sc accelerating structure is a 352.21 MHz spoke resonator section, followed after a frequency jump to 704.42 MHz, by two families of elliptical multicell cavities.

The sc LINAC is responsible for 98% of the energy gain and covers around 90% of the LINAC length. The purpose of this study is to find the optimum number of spokes and cells in each of these three families, as well as the best geometric βs, number of cavities per period and finally the transition energy between the neighboring structures.

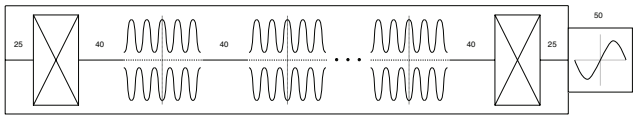

Figure 1: Simplified diagram of the cryomodule layout used in this study; Hybrid cryo-module. *the numbers are in cm in this figure.*

Since all of these parameters depend on each other, the optimization has to be performed in an 8 dimensional space: 3D of β_gs, 3D of number of cavities per cryomodule, and 2D of transition energy between spokes to low β and from low β to high β. The number of spokes in spoke resonators, as well as the number of cells in elliptical cavities, is fixed to 2 and 5 respectively by a previous study [3].

An example of a simple cryomodule for the hybrid design is presented in Fig. 1. The drawing shows the structure, as well as the distances between the active elements of the LINAC for the low β and high β cryomodules. This spacings though plausible, are preliminary values. They must be optimized to fulfill cryogenics, diagnostics, and rf requirements in order not to cause any extra heat load, lack of space for diagnostics or rf coupling between neighboring cavities.

POWER, VOLTAGE, AND PHASE SETTINGS

Choice of Accelerating Gradients

Choosing the right accelerating gradient is of great importance, since an over specified value will result in a LINAC which will be shorter on paper, but will not be able to bring the beam to its final energy if the gradient can't be achieved. On the other hand an underspecified value may result in a LINAC which will be unnecessarily long and expensive. The process of finding the optimum accelerating gradient is explained in [3], resulting in a gradient proportional to β_g of the cavity through:

$$E_{acc} = E_{surface}/(1.95/\beta_g + 1.15 \cdot \beta_g - 1), \qquad (1)$$

where $E_{surface}$ is the peak electric surface field on the cavity surface, being fixed to 40 MV/m, based on [4]. The accelerating gradient vs. cavity is plotted in Fig. 2.

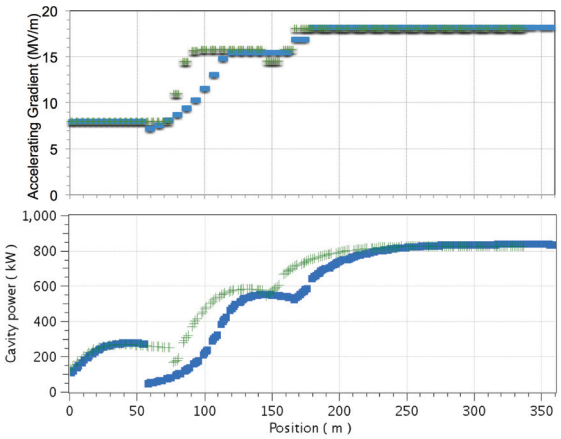

Figure 2: Top: Accelerating gradient along the SC LINAC, Bottom: The required power per cavity along the SC LINAC. Green: discontinuous phase advance variation between Spoke and low β, Blue: Continuous phase advance.

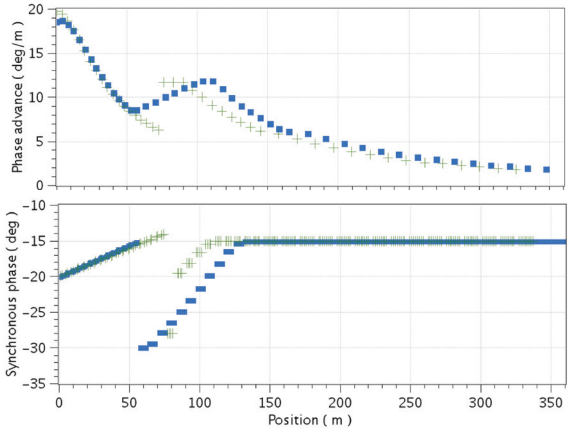

Figure 3: Top: Phase advance per meter along the SC LINAC, Bottom: Synchronous phase along the SC LINAC, Green: Step, Blue: Smooth.

Power

For the ESS beam current of 50 mA and an accelerating gradient of ~20 MV/m, the required power to accelerate the beam would be ~1 MW for a cavity which is almost 1 m long, in case we neglect the synchronous phase. At such a high power, around ~1 MW per coupler, rf windows have to be designed carefully due to the high thermo-mechanical stresses which they have to endure. A pair of such couplers capable of delivering up to ~1.2 MW, at 50 Hz and for a 2 ms pulse has been built and tested in Saclay, France. [5].

Accelerating rf phase

Acceleration and bunching of the continuous beam of particles out of source starts in the RFQ at $-90°$ and then gradually increases to $-20°$ at the end of DTL. Since the frequency stays the same in the spokes, the accelerating phase starts at $-20°$ and increases by $0.18°$ per cavity to reach almost $-14°$ in the very last spoke resonators, except for the matching cavities. Elliptical cavities will work at twice the spoke frequency, i.e. 704.42 MHz, and if this frequency jump is not handled correctly a loss of longitudinal acceptance in the transition may cause excessive emittance increase and/or particle loss in the elliptical cavities. Accelerating phase as well as accelerating gradient are decreased in the first few periods of the elliptical cavities [6] to keep the bucket size constant, and the synchronous phase is gradually increased to $-15°$.

Longitudinal Phase Advance

Another boundary condition of the optimization process is the limit on the longitudinal phase advance per period. The upper limit chosen during this study is $80°$ per period, to allow for a minimum transverse to longitudinal phase advance ratio of 1.125. If we do not limit the phase advance variation between spoke resonators and low β cavities, there will be a step like discontinuity in average phase advance, phase advance per meter, due to the frequency jump, "Step" in Fig. 3. This may decrease the beam dynamics performance of the machine and act as a bottle neck. To avoid this, the maximum longitudinal phase advance variation per period is limited to $0.5°$ per meter. In the study this case is labeled as "Smooth", Fig. 3.

HYBRID DESIGN

A new type of hybrid cryomodule architecture is proposed and is under study, allowing for a transition between cryomodules in the sub-100 K region. The advantages of the new hybrid design are that it will generate a lower heat load with respect to a fully segmented design, while still providing easy access to individual cryomodules for maintenance and repair. It also allows for independent alignment of the quadrupoles, which are mounted at the two extremities of the cryomodule, e.g. using LHC type three axes alignment jacks [8]. It has many of the advantages of a continuous cold design. The fact that such a design will be longer should not be considered without noting that it has the extra 500 mm area reserved for devices, such as beam instruments, vacuum gauges, et cetera. This option is called hybrid, since it uses two ranges of temperatures and is a mixture between continuous and segmented design.

In entirely segmented cryomodules, an important part of the static heat load stems from sub-optimal screening at the cold-warm transitions. By cooling down the utility block to screen temperature, i.e. around 70 K, this heat load can be significantly reduced. The cooldown is achieved by fitting a vacuum jacket around the utility block, thus creating a separate utility module and by fitting this module with a 70 K thermal screen. This screen is supplied with cold helium from one of the adjacent cryomodules' screen circuits. A dedicated vacuum pump assures the insulating vacuum. The exact thermal benefits of this solution are being evaluated and will be weighed against the drawbacks, which are

Table 1: Optimized values for hybrid design. The accelerating gradient varies as a function of β_g as in eq. 1.

	STEP	SMOOTH
β_g / E_{acc}(MV/m)	0.55 / 8	0.57 / 8
Final energy (MeV)	234	188
Cav./Per. $\times$ N_{period}	2×19	2×14
β_g / E_{acc}(MV/m)	0.72 / 15.77	0.70 / 15.44
Final energy (MeV)	612	606
Cav./Per. $\times$ N_{period}	4×10	4×16
β_g / E_{acc}(MV/m)	0.89 / 18.06	0.90 / 18.17
Final energy (MeV)	2500.8	2505.6
Cav./Per. $\times$ N_{period}	8×15	8×15
No. of Cavities / Periods	198 / 44	212 / 45
REG (MeV/m)	7.369	6.938
Length (m)	340.859	362.552

From top to bottom: Spokes, Low β, High β, and Total.

namely increased equipment costs and increased heat load on the 70 K screen. There are still many design issues to be resolved, such as the exact mechanical and cryogenic setup of the utility module. The design solutions have in turn an influence on thermal screening efficiency and cryogenic losses. A number of iterations are foreseen in order to optimize these parameters. The basic design of a cryomodule with provisions for allowing utility block cooling is not in contradiction with a standard segmented cryomodule design. Therefore, a later decision against utility block cooldown could be taken without any negative consequences to the cryomodule design process.

RESULTS

Two sets of optimizations, smooth and stepwise phase advance variation between spoke and low β, are performed for these superconducting LINACs, by using equation 1 to calculate the field for each geometric β. In the simulations the output energy of the DTL is set to 49.5 MeV, to compensate for a possible lower energy due to matching. An accelerating field of 8 MV/m is chosen in the spoke resonators. A surface peak field of 40 MV/m is used for the elliptical cavities. Accelerating gradient in each cavity is presented in Table 1. The code GENLINWIN, [10], is used to calculate and find the optimized LINAC.

A set of preliminary beam dynamics simulations was performed to allow a comparison of the structures from the beam dynamics performance point of view, using the code TRACEWIN [10]. The transverse phase advance follows the longitudinal phase advance with a transverse to longitudinal ratio of 1.125. A beam of 100,000 multi particles was generated using a Gaussian distribution cut at three sigma at the entrance to the superconducting LINAC. The beam is matched to the structure from DTL. Matching between structures is done using one pair of quadrupoles and a maximum of four cavities on each side. To check the sensitivity of different designs in a fast (not necessarily precise) way, an

Table 2: Beam dynamics performance summary.

	Mismatch	Step		Smooth	
	(%)	$\Delta\epsilon^{\dagger}$[%]	$\delta H^{\ddagger}$	$\Delta\epsilon$[%]	δH
X	0	17.4	0.434	14.3	0.291
Y	0	22.2	0.388	19.4	0.290
Z	0	5.0	0.250	5.9	0.298
X	50	118.3	3.588	122.2	3.416
Y	50	125.8	3.106	111.8	3.313
Z	50	88.3	2.348	85.2	2.498

† : $\Delta\epsilon = (\epsilon_f - \epsilon_i)/\epsilon_i$, ‡ : $\delta H = H_f - H_i$

initial mismatch is applied to the beam by increasing the Twiss parameters, i.e.

$$\begin{aligned} \alpha_{\text{mismatch}} &= \alpha_{\text{match}} \times 2.25, \\ \beta_{\text{mismatch}} &= \beta_{\text{match}} \times 2.25, \end{aligned} \tag{2}$$

in all the three planes to have a mismatch of 50% at injection. The beam is then tracked along the LINAC without rematching between the structures. The main part of transverse emittance growth is due to space charge force dominated redistribution of particles inside beam, which happens in the first three periods. It is worth mentioning that all the losses in all the lossy runs happen in the second doublet in the line, where the beam is transversally very large after going through a waist in the middle of the first period.

CONCLUSION

The new hybrid structure is studied and an optimized LINAC with the same criteria is designed and compared to the two previously designed superconducting LINACs with cold and warm quadrupoles. The hybrid LINAC is comparable in every sense, excluding the fact that it is longer. It also has the advantage of better alignment of quadrupoles, and it is the most flexible with respect to required diagnostics.

REFERENCES

[1] M. Eshraqi, et. al., Proceedings of HB2010, Morschach, Switzerland, September 2010.

[2] "ESS Volume III Update: Technical report status", 2003.

[3] M. Eshraqi, ESS AD Technical Note, ESS/AD/0010.

[4] P. Pierini, "Analysis of gradients for proton linac", Gradients and Betas for ESS LINAC, Lund, September 2010, Sweden.

[5] G. Devanz, et. al., Proceedings of SRF2009, Berlin, 2009, Germany.

[6] R. Duperrier, N. Pichoff, and D. Uriot, Phys. Rev. ST Accel. Beams, **10**, 084201, (2007).

[7] R. Stanek, "Linac Proton Driver Cost Estimate".

[8] J. Dwivedi, et. al., "The Alignment Jacks of the LHC", Proceedings of EPAC04, Lucerne, 2004, Switzerland.

[9] D. Ene, et. al. "Radiation protection Studies for ESS Superconducting Linear Accelerator", *to be published.*

[10] R. Duperrier, N. Pichoff and D. Uriot, Proceedings of ICCS02, Amsterdam, The Netherlands, 2002.